Optimal Resource Allocation for Fast Epidemic Monitoring in Networked Populations

Paolo Di Giamberardino[1][a], Daniela Iacoviello[1][b] and Federico Papa[2]
[1]*Dept. of Computer, Control and Management Engineering A.Ruberti, Sapienza University of Rome, Rome, Italy*
[2]*IASI, CNR, Rome, Italy*

Keywords: Epidemic Modeling, Optimal Resource Allocation, Monitoring.

Abstract: The COVID-19 pandemic highlighted the fragility of the world in addressing a global health threat. The available resources of the pre-pandemic national health systems were inadequate to cope with the huge number of infected subjects needing health care and with the rapidity of the infection spread characterizing the COVID-19 outbreak. Indeed, an adequate allocation of the resources could produce in principle a strong reduction of the infection spread and of the hospital burden, preventing the collapse of the health system. In this work, taking inspiration from the COVID-19 and the difficulties in facing the emergency, an optimal problem of resource allocation is formulated on the basis of an ODE multi-group model composed by a network of SEIR-like submodels. The multi-group structure allows to differentiate the epidemic response of different populations or of various subgroups in the same population. In fact, an epidemic does not affect all populations in the same way, and even within the same population there can be epidemiological differences, like the susceptibility to the virus, the level of infectivity of the infectious subjects and the recovery from the disease. The subgroups are selected within the total population based on some peculiar characteristics, like for instance age, work, social condition, geographical position, etc., and they are connected by a network of contacts that allows the virus circulation within and among the groups. The proposed optimal control problem aims at defining a suitable monitoring campaign that is able to optimally allocate the number of swab tests between the subgroups of the population in order to reduce the number of infected patients (especially the most fragile ones) so reducing the epidemic impact on the health system. The proposed monitoring strategy can be applied both during the most critical phases of the emergency and in endemic conditions, when an active surveillance could be crucial for preventing the contagion rise.

1 INTRODUCTION

The COVID-19 pandemic has been modifying the habits all over the world, inducing all the populations to apply containment measures, such as social distancing, using masks, participating to swab test campaigns, and getting the vaccination when it became available. A huge amount of papers have been published on this topic, focusing on the effects and the effectiveness of such actions, see (Gatto et al., 2020), (Di Giamberardino and Iacoviello, 2021), (Pung et al., 2021), (Casares and Khan, 2020), (Espinoza et al., 2020), (Liu et al., 2020), (Borri et al., 2021) only as possible examples. In literature, different aspects have been investigated, changing the focus of the analysis as the pandemic conditions vary, ranging from data analysis in the very first period of the emergency, (Tang et al., 2020), (Wu et al., 2020), to modeling and control during $2020-2021$, (Ivorra et al., 2020), (Wang et al., 2020), (Silva et al., 2021), (Di Giamberardino et al., 2021b) up to ex-post analysis of what happened, in order to understand the dynamics of the infections and to avoid possible delays in decision making in case of new sanitary emergencies, (Assefa et al., 2022), (Marziano et al., 2021), (Di Giamberardino et al., 2021a). The main COVID-19 specificities are the high infection rate, the significant percentage of asymptomatic subjects that can infect, the different course of the illness in the various categories, and not well identified reasons of sensitivity with respect to the disease. The strong relationships among populations, and inside each population, increase the probability of new infections and therefore of the epidemic spread. The spread among

[a] https://orcid.org/0000-0002-9113-8608
[b] https://orcid.org/0000-0003-3506-1455

Di Giamberardino, P., Iacoviello, D. and Papa, F.
Optimal Resource Allocation for Fast Epidemic Monitoring in Networked Populations.
DOI: 10.5220/0011299300003271
In *Proceedings of the 19th International Conference on Informatics in Control, Automation and Robotics (ICINCO 2022)*, pages 616-625
ISBN: 978-989-758-585-2; ISSN: 2184-2809

populations is studied in (Di Giamberardino et al., 2021) where the mobility aspects after the lockdown of 2020 in Italy are analysed; in that case the entire Italian population has been split into three geographical groups (referring to North, Center and South of Italy) showing the influence of controlled re-opening, after the lockdown, on the distribution of the infection. The connections among groups of populations can be faced considering as "population" not only the habitants of a region but also, for example, a category of workers, or an age-category; therefore, it is possible to study the interconnections among social groups with different characteristics, analysing the effects, on the entire population, of control actions applied separately in one group, (Contreras et al., 2020), (Di Giamberardino et al., 2021), (Ndairou et al., 2020). At the very beginning of the current pandemic, the available resources were not sufficient for the severity of the emergency and some choices had to be taken. In absence of vaccination and ad hoc medications, two main containment measures are, in general, achievable: the social distancing (including the use of masks) and the fast identification of infected patients. This latter issue can be fulfilled by means of an adequate monitoring campaign based on swab tests, which were not easily available at the beginning of the COVID-19 pandemic. Moreover, also in the endemic condition, an active surveillance action could consider a regular swab test campaign to contain the number of infected patients, especially in the most fragile part of the population. The main goal of this paper is to propose a strategy for optimizing the swab test campaign, considering also limitations from logistic, economic and material points of view.

The paper is organized as follows. In Section 2, the total population is divided into n groups and a compartmental model describing the disease dynamics in each group is proposed and analysed. An optimal allocation control is proposed, which aims at yielding a strategy for defining a swab test campaign in case of limited resources, both from economic and technical point of view. In Section 3, the introduction of the optimized strategy for fast epidemic monitoring is studied, comparing its effects with the non controlled case. Conclusion and future developments end the paper.

2 MATERIALS AND METHODS

A population is here modeled as partitioned into n groups; this could represent, for example, a classification with respect to the age, or to the geographical position, or to the working categories, or any other characteristics that imply different response to the virus. In each group, 7 compartments representing different patient conditions w.r.t. the disease evolution are introduced. In particular, the severity of the disease is explicitly taken into account by distinguishing between asymptomatic (A) and symptomatic isolated infected (I), and hospitalized (H) individuals. This choice depends on the COVID-19 specificity characterized by an high percentage of asymptomatic patients that could infect other people and by the high heterogeneity of the disease severity, going from the absence of symptoms to the need of health assistance.

In the following, three subsections will be developed; in the first one the mathematical model is proposed; then, the reproduction number is determined analysing the system by means of the next generation matrix approach. Finally, the control problem aiming at the optimal resource allocation is introduced. The optimal strategy addresses the fast identification of asymptomatic patients to reduce, as soon as possible, new infections and hospitalizations.

2.1 Mathematical Model

As previously said, each group is partitioned into 7 compartments as shown by Fig. 1. So, referring to the h–th group, $h = 1, \ldots, n$, the model accounts for the following compartments:

- S_h: susceptible subjects, that is the healthy people within the population which are not vaccinated yet;
- E_h: exposed individuals, i.e. the subjects in the incubation period; they are infected but cannot infect;
- I_h: infected isolated patients; this compartment collects infected patients who are diagnosed as COVID-19 positive (because of the presence of recognizable symptoms or of a positive swab test). As diagnosed patients, they are isolated and cannot transmit the infection;
- H_h: isolated hospitalized patients; it is assumed that they are isolated in hospital, with serious health conditions;
- A_h: infected non isolated patients; they are subjects unaware of their infection status, since they show only light or no symptoms at all; therefore, they can infect other people of the same or of different groups;
- R_h: removed subjects, immunized because of the healing from the infection; they are aware of their previous infection status;

- R_{Ah}: removed subjects, immunized because of the healing from the infection; they are unaware of their previous infection status.

Note that the immunization assumed for compartments R_h and R_{Ah} is actually a temporary condition that could be reached after healing, and its presence and duration substantially depend on the particular virus strain that is dominant within the infected population. Since the majority of virus strains appeared during the COVID-19 evolution have produced some transitory protection from the reinfection, it is reasonable to assume a sort of immunization in the problem formulation, at least for a short period after the recovery. Note also that the distinction among the healed patients between those aware of their previous infection state (R_h) and those unaware (R_{Ah}), allows to exclude the first class R_h from the swab test campaign, at least until few months after healing. The class of people indicated by R_{Ah} is not measurable, of course, as the class of A_h, but they could be approximately inferred from some extrapolation based on the test results related to specific populations or to particular periods.

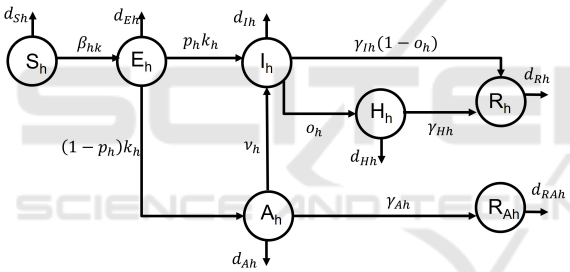

Figure 1: Block diagram of the proposed model for the h–th group.

It is assumed that only the subjects in the class A_h of each group h can infect the subjects S_j of any group j. Therefore, it is mandatory to recognize as soon as possible the subjects in each class A_h, $h = 1,\ldots,n$, by means of a suitable swab test campaign, taking into account the operative limitations.

The unique subjects really sure of their health conditions are the ones that have received a positive diagnosis of COVID-19 after a swab test and/or after having developed the symptoms, i.e. the subjects in the classes I_h, H_h and R_h, whereas the remaining ones in the classes S_h, E_h, A_h and R_{Ah} need to be tested. After a test, the subjects in S_h and R_{Ah} don't change their class, whereas the subjects in E_h and A_h move to I_h; this justifies the weight coefficient $\frac{\rho_h E_h}{S_h+E_h+A_h+R_{Ah}}$ of the control action term influencing the subjects in E_h and, correspondingly, the weight $\frac{\tau_h A_h}{S_h+E_h+A_h+R_{Ah}}$ regarding the evolution of A_h.

The dynamic equations describing the epidemic spread of each group h can be written as

$$\dot{S}_h = N_h - S_h \sum_{k=1}^{n} \beta_{hk} A_k - d_{Sh} S_h \tag{1}$$

$$\dot{E}_h = S_h \sum_{k=1}^{n} \beta_{hk} A_k - d_{Eh} E_h - k_h E_h - \frac{\rho_h E_h}{S_h + E_h + A_h + R_{Ah}} u_h \tag{2}$$

$$\dot{I}_h = -d_{Ih} I_h + p_h k_h E_h - \gamma_{Ih}(1-o_h) I_h + \nu_h A_h + \frac{\rho_h E_h + \tau_h A_h}{S_h + E_h + A_h + R_{Ah}} u_h - o_h \bar{o}_h I_h \tag{3}$$

$$\dot{A}_h = -d_{Ah} A_h + (1-p_h) k_h E_h - \gamma_{Ah} A_h - \nu_h A_h - \frac{\tau_h A_h}{S_h + E_h + A_h + R_{Ah}} u_h \tag{4}$$

$$\dot{H}_h = -d_{Hh} H_h - \gamma_{Hh} H_h + o_h \bar{o}_h I_h \tag{5}$$

$$\dot{R}_h = -d_{Rh} R_h + \gamma_{Ih}(1-o_h) I_h + \gamma_{Hh} H_h \tag{6}$$

$$\dot{R}_{Ah} = -d_{RAh} R_{Ah} + \gamma_{Ah} A_h \tag{7}$$

The parameters appearing as coefficients in (1)–(7) have the following meanings:

- d_{*h} denotes the death rate in compartment $*$ of the $h-th$ group;
- $\frac{1}{k_h}$ is the mean incubation time in E_h;
- β_{ij} represents the infection rate constant between the healthy subjects S_i and the infectious ones A_j, with $i = 1,..,n$, $j = 1,...,n$;
- $\frac{1}{\nu_h}$ is the mean period of natural transition from A_h to I_h;
- $\frac{1}{\bar{o}_h}$ represents the mean period required for an infected patient to be hospitalized, i.e. to transit in H_h; it is assumed that it is immediately evident that the patient is in need of hospitalization; in the following this value will be set equal to 1;
- $\frac{1}{\gamma_{A_h}}$, $\frac{1}{\gamma_{I_h}}$ and $\frac{1}{\gamma_{H_h}}$ represent the mean periods required for the healing of patients in the classes A_h, I_h and, respectively, H_h;
- ρ_h and τ_h are normalization coefficients related with the reliability of the swab tests;
- $p_h \in [0,1]$ is the probability that a subject in E_h becomes an infected patient in I_h after developing COVID-19 symptoms;
- $o_h \in [0,1]$ is the probability that a subject in I_h requires hospitalization because of health worsening;

- N_h represents the rate of new incomers.

The different n groups influence each other by means of the infection rates depending on the peculiarities of the population at hand. In the following, the total model of the n groups is analysed, finding, in particular, the expression of the reproduction number R_0.

2.2 Model Analysis

This model will be analysed considering the whole population with the n groups connected; the state of the h-th group is denoted by

$$X_h = \begin{pmatrix} S_h & E_h & I_h & A_h & H_h & R_h & R_{Ah} \end{pmatrix}^T \quad (8)$$

Therefore, setting X as the $7n$–dimensional column vector

$$X = \begin{pmatrix} X_1 \\ X_2 \\ \vdots \\ X_n \end{pmatrix}$$

and observing that the equations describing the trend of each group depend on all the state variables of all the groups (because of the infection mechanism sustained by the asymptomatic subjects), the h–th dynamical system can be written as

$$\dot{X}_h = \Gamma_h(X) + \Omega_h(X_h)u_h \quad (9)$$

with the obvious meaning of the notation, and the global system can be described as

$$\dot{X} = \Gamma(X) + \Omega(X)U \quad (10)$$

In (10)

$$\Gamma(X) = \begin{pmatrix} \Gamma_1(X) \\ \vdots \\ \Gamma_n(X) \end{pmatrix} \quad (11)$$

is the $7n \times 1$ vector function representing the non controlled part of the state equations, while $\Omega(X)$ is the $7n \times n$ matrix

$$\Omega(X) = \begin{pmatrix} \Omega_1(X_1) \cdots & 0 \\ \vdots & \ddots & \vdots \\ 0 & \cdots \Omega_n(X_n) \end{pmatrix} \quad (12)$$

multiplying the control vector

$$U = \begin{pmatrix} u_1 & u_2 & \dots & u_n \end{pmatrix}^T$$

The disease free equilibrium point

$$P^e = \begin{pmatrix} P_1^e \\ P_2^e \\ \vdots P_n^e \end{pmatrix}$$

is easily obtained and it is given by

$$P_h^e = \begin{pmatrix} S_h^e & 0 & 0 & 0 & 0 & 0 & 0 \end{pmatrix}^T$$

with $S_h^e = \frac{N_h}{d_{S_h}}$.

A useful parameter that provides information on the evolution of the pandemic, in the absence of control actions, is the reproduction number $\mathcal{R}_0$, that is the mean number of secondary cases per unit time that a unique infected subject produces in a totally susceptible population. An estimation of $\mathcal{R}_0$ can be obtained by means of the next generation matrix method, (Van Den Driessche and Watmough, 2002); it requires the definition of the vector Z that collects the variables of the global system describing the evolution of the infected people (in all the phases) in the whole population

$$Z = \begin{pmatrix} Z_1 \\ Z_2 \\ \vdots \\ Z_n \end{pmatrix}$$

where

$$Z_h = \begin{pmatrix} E_h & I_h & A_h & H_h \end{pmatrix}^T$$

The reduced dynamical system $\dot{Z}$ can be described by distinguishing the terms that include new infections ($\mathcal{F}$) from all other changes ($\mathcal{V}$) in the population

$$\dot{Z} = \mathcal{F} - \mathcal{V}$$

where

$$\mathcal{F} = \begin{pmatrix} \mathcal{F}_1 \\ \mathcal{F}_2 \\ \vdots \\ \mathcal{F}_n \end{pmatrix} \qquad \mathcal{V} = \begin{pmatrix} \mathcal{V}_1 \\ \mathcal{V}_2 \\ \vdots \\ \mathcal{V}_n \end{pmatrix}$$

with

$$\mathcal{F}_h = \begin{pmatrix} S_h \sum_{k=1}^n \beta_{hk} A_k \\ 0 \\ 0 \\ 0 \end{pmatrix}$$

$$\mathcal{V}_h = \begin{pmatrix} d_{Eh}E_h + k_h E_h \\ d_{Ih}I_h - p_h k_h E_h + \gamma_{Ih}(1-o_h)I_h - \nu_h A_h \\ d_{Ah}A_h - (1-p_h)k_h E_h + \nu_h A_h + \gamma_{Ah}A_h \\ d_{Hh}H_h + \gamma_{Hh}H_h - o_h I_h \end{pmatrix}$$

Starting from $\mathcal{F}$ and $\mathcal{V}$, new matrices, say F and V, are defined as follows

$$F = \left(\frac{\partial \mathcal{F}}{\partial Z}\right)_{P^e} = \begin{pmatrix} F_{1,1} \cdots F_{1,n} \\ \vdots \ddots \vdots \\ F_{n,1} \cdots F_{n,n} \end{pmatrix} \quad (13)$$

where

$$F_{h,j} = \left.\frac{\partial \mathcal{F}_h}{\partial Z_j}\right|_{P^e} = \begin{pmatrix} 0 & 0 & S_h^e \beta_{hj} & 0 \\ 0 & 0 & 0 & 0 \\ 0 & 0 & 0 & 0 \\ 0 & 0 & 0 & 0 \end{pmatrix} \quad (14)$$

and

$$V = \left(\frac{\partial \mathcal{V}}{\partial Z}\right)_{P^e} \quad (15)$$

The matrix V, of dimension $4n \times 4n$, is block diagonal with the non null blocks equal to

$$V_{jj} = \begin{pmatrix} d_{Eh}+k_h & 0 & 0 & 0 \\ -p_h k_h & d_{Ih}+\gamma_{Ih}(1-o_h) & -\nu_h & 0 \\ -(1-p_h)k_h & 0 & d_{Ah}+\gamma_{A_h}+\nu_h & 0 \\ 0 & -o_h & 0 & d_{Hh}+\gamma_{Hh} \end{pmatrix}$$

The reproduction number $\mathcal{R}_0$ is defined as the dominant eigenvalue of the next generation matrix FV^{-1}. Due to the diagonal block structure of the next generation matrix, the reproduction number $\mathcal{R}_0$ is the maximum of the set $\{\mathcal{R}_{0h}\}$, $h = 1,...,n$, where $\mathcal{R}_{0h}$ is the reproduction number of group h and it is given by

$$\mathcal{R}_{0h} = \frac{S_h^e \beta_{hh}(1-p_h)k_h}{(d_{Eh}+k_h)(d_{Ah}+\gamma_{Ah}+\nu_h)} \quad (16)$$

This implies that, if we consider the entire population constituted by the n interacting groups, the total reproduction number $\mathcal{R}_0$ is less than 1, thus leading to the reduction of the pandemic, if and only if the reproduction number of each group $\mathcal{R}_{0h}$, $h = 1,...,n$, is smaller than 1. Note that each $\mathcal{R}_{0h}$, $h = 1,...,n$, increases with β_{hh} and with $(1-p_h)$; this is due to the fact that the unique population that could infect is constituted by the asymptomatic subjects in A_h, that, in fact, increase as $(1-p_h)$ does.

2.3 Optimal Control

In a pandemic scenario characterized by a severe limitation on the swab test availability, like for instance in the first phase of the epidemic outbreak or during a prolonged surveillance strategy, it is mandatory to optimally allocate the available resources to decrease the total number of infected patients (infected, asymptomatic, hospitalized). The following cost index is proposed

$$\begin{aligned} J(U) &= \int_{t_i}^{t_f} L(X,U)dt \\ &= \frac{1}{2}\int_{t_i}^{t_f} \sum_{k=1}^{n} [\alpha_k^A A_k^2 + \alpha_k^I I_k^2 + \alpha_k^H H_k^2 + \mu_k u_k^2]dt \end{aligned}$$

with the constraints

$$u_k \in [u_k^m, u_k^M], \qquad u_k^m < u_k^M, \qquad k = 1,\dots,n$$

The weights α_k^A, α_k^I, α_k^H are chosen between 0 and 1 depending on the relative importance of the various terms. The use of the Pontryagin principle requires the introduction of the $7n$-dimension costate vector, $\Lambda = (\lambda_1 \quad ... \quad \lambda_{7n})^T$, satisfying the costate vectorial equation

$$\dot{\Lambda} = -\left.\frac{\partial \mathcal{H}}{\partial X}\right|^T \quad (17)$$

being $\mathcal{H}$ the Hamiltonian of the process

$$\mathcal{H}(X,U) = L(X,U) + \Lambda^T[\Gamma(X) + \Omega(X)U] \quad (18)$$

According to the Pontryagin inequality, the optimal control action u_h^o of group h satisfies the condition:

$$\begin{aligned} &\frac{1}{2}\mu_h u_h^{o2} + \sum_{j=2}^{4} \lambda_{7(h-1)+j}\Omega_{7(h-1)+j,h}u_h^o \\ &\leq \frac{1}{2}\mu_h w_h^2 + \sum_{j=2}^{4} \lambda_{7(h-1)+j}\Omega_{7(h-1)+j,h}w_h \end{aligned} \quad (19)$$

for any admissible control $w_h \in [u_h^m, u_h^M]$. The quantity $\Omega_{l,m}$ denotes the the row l and the column m of the matrix Ω defined in (12).

Therefore, the n optimal control actions are equal to

$$u_h^o(t) = \Phi_h(t), \quad h = 1,\dots,n, \quad (20)$$

where

$$\begin{aligned} \Phi_h(t) &= \frac{-\sum_{j=2}^{4} \lambda_{7(h-1)+j}\Omega_{7(h-1)+j,h}}{\mu_h} \\ &= -\frac{1}{\mu_h}\left[-\lambda_{7(h-1)+2}\frac{\rho_h E_h}{S_h+E_h+A_h+R_{Ah}}\right. \\ &\quad +\lambda_{7(h-1)+3}\frac{\rho_h E_h + \tau_h A_h}{S_h+E_h+A_h+R_{Ah}} \\ &\quad \left. -\lambda_{7(h-1)+4}\frac{\tau_h A_h}{S_h+E_h+A_h+R_{Ah}}\right] \end{aligned} \quad (21)$$

whenever $\Phi_h(t)$ is in $[u_h^m, u_h^M]$. Otherwise, if $\Phi_h(t) \geq u_h^M$ or $\Phi_h(t) \leq u_h^m$ the optimal control is given by u_h^M or, respectively, u_i^m.

Note that, as usual, the switching functions $\Phi_h(t)$ depend on the costate evolution, given by Eq. (17) solved backward starting from the final condition $\Lambda(t_f) = 0$.

3 NUMERICAL RESULTS

In this section it is analysed the epidemic trend of a simulated population in which, for its peculiarities, four different groups can be identified; these groups may be differentiated based on their weakness and susceptibility with respect to the virus infection and on different healing capability. It may correspond to age-class subdivision or activity-related differences; the four groups, referred for simplicity as G_i, $i = 1,2,3,4$, are defined by the initial conditions given in Table 1 and by the model parameters given in Tables 2, 3. Each control u_h is limited by the box constraint $[0.05, 0.99]$. Fig.2 shows the network regarding the infection spread within the population with the 4 selected groups. The scenario described in

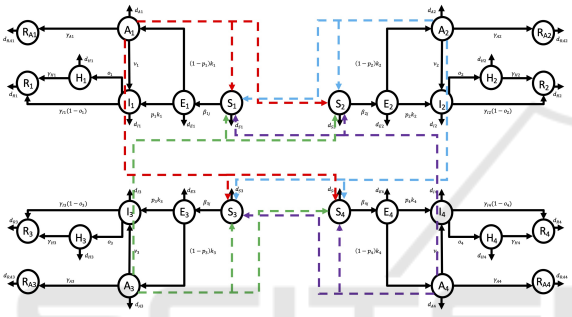

Figure 2: Virus spread in a network of 4 connected groups.

this paper assumes that group G_1 has a higher infection capability with respect to the others; this means that the contact rates β_{i1} for $i = 1,...,4$ are higher with respect to the other values of the matrix β collecting the contact rates β_{ij}, $i, j = 1,...,4$

$$\beta = 10^{-7} \begin{pmatrix} 9.5 & 7 & 5 & 2 \\ 9.4 & 8 & 7 & 4 \\ 9.4 & 5 & 8 & 7 \\ 9.8 & 5 & 7 & 8 \end{pmatrix} \tag{22}$$

Among the groups G_i, $i = 1,...,4$, it is assumed a decreasing capability of healing from the infection, as well as an increasing probability of hospitalization after the infection, as i increases (see Tables 2, 3). The described situation could correspond to a possible splitting of the population into 4 groups depending on age; therefore, as the age increases the subjects of each group become more susceptible to the infection, weaker and with increased probability of hospitalization. The rate of new incomers in each S_h is estimated as $S_h(0) \cdot d_{Sh} \cdot 100$, that is 100 times the corresponding death rate.

The choice of the weights in the cost index depends on the specific goal to be pursued. In the considered scenario, the aim is to minimize the infected subjects allocating optimally the available resources, that is defining the optimal planning of the swab test campaign, which is very useful in case of resource limitation, especially at the beginning of a sanitary emergency but also for a prolonged surveillance, during and after the pandemic and endemic period. As said, group G_1 includes subjects with higher infectious capability and lower probability of showing symptoms; therefore, a possible goal is to decrease the number of patients in A_1; at the same time, it is mandatory to avoid the infection and hospitalization of the weak subjects. With this framework in mind, the values in Table 4 are proposed.

Table 1: Initial conditions.

	G_1	G_2	G_3	G_4
$S_i(0)$	10^6	$3 \cdot 10^6$	$4.5 \cdot 10^6$	10^6
$E_i(0)$	10^2	$4 \cdot 10^2$	$3 \cdot 10^3$	$2 \cdot 10^2$
$I_i(0)$	50	10	20	4
$A_i(0)$	10^2	3	5	10
$H_i(0)$	10	10	10	$5 \cdot 10^2$
$R_i(0)$	10^2	$4 \cdot 10^3$	10^3	$2 \cdot 10^2$
$R_{Ai}(0)$	$5 \cdot 10^2$	10^2	$8 \cdot 10^2$	10^2

Table 2: Death rated parameters for each group $i = 1...,4$; note that the values in the table must be multiplied by 10^{-5}.

	G_1	G_2	G_3	G_4
$d_{Si} \cdot 10^5$	1	1.5	1.5	2
$d_{Ei} \cdot 10^5$	1	1.5	1.5	2.3
$d_{Ii} \cdot 10^5$	1.1	1.7	1.8	3
$d_{Ai} \cdot 10^5$	1.02	1.5	1.6	3.4
$d_{Hi} \cdot 10^5$	1.2	1.8	1.8	4
$d_{Ri} \cdot 10^5$	1	1.5	1.5	1.5
$d_{RAi} \cdot 10^5$	1	1.5	1.5	2

As far as the control weights, without specific reasons for privileging the action over one category, it was decided to weigh the controls u_h, $h = 1,...4$ in the same way, assuming $\mu_k = 0.5 \cdot 10^5$ for $k = 1,...,4$. Note the different order of magnitude of the weights of the state variables and of the controls; this is due to make these quantities comparable and effective in the cost index. The simulations are obtained over a period of 60 days, with a sampling time of 0.5. With the chosen parameters, it can be noted the suggested strategy, Fig. 3; by using the maximum allowed effort for the swab test campaign in G_1 for about 93% of the control period, it is possible to apply the control on groups G_2, G_3 and G_4 for about 80%, 70% and, respectively, 65% of the control period. These choices produce a reduced increase in the trends of asymptomatic, infected and hospitalized patients, as shown in Figs.4, 5, 6. It can be noted, especially for the subjects in G_2 and G_3, an increase in the number of asymptomatic subjects after the end of the swab test campaign, but a

Table 3: Model parameters for each group $i = 1...,4$.

	G_1	G_2	G_3	G_4
k_i	$\frac{1}{6}$	$\frac{1}{6}$	$\frac{1}{6}$	$\frac{1}{6}$
ρ_i	10^6	10^6	10^6	10^6
p_i	0.1	0.5	0.7	0.85
ν_i	$\frac{1}{5}$	$\frac{1}{4}$	$\frac{1}{3}$	$\frac{1}{2}$
τ_i	10^4	10^4	10^4	10^4
o_i	0.1	0.4	0.6	0.8
γ_{A_i}	$\frac{1}{7}$	$\frac{1}{8}$	$\frac{1}{9}$	$\frac{1}{14}$
γ_{H_i}	$\frac{1}{7}$	$\frac{1}{8}$	$\frac{1}{9}$	$\frac{1}{14}$
γ_{I_i}	$\frac{1}{7}$	$\frac{1}{8}$	$\frac{1}{9}$	$\frac{1}{14}$

Table 4: Choice of the weights in the cost index.

	G_1	G_2	G_3	G_4
α_k^A	0.99	0.08	0.02	0.008
α_k^I	0.04	0.05	0.08	0.1
α_k^H	0.4	0.5	0.7	0.99

general decrease, or at least not increasing trend, for the infected patients in all the groups. To check the effects of the application of the optimal controls u_i^o, $i = 1,...,4$ to the overall infectious situation, in Fig. 7 the total number of infected and infectious subjects (that is all the infected, asymptomatic and hospitalized patients) is shown, both with the application of the obtained optimal control (continuous line) and in free evolution (dashed line). It can be noted that the controlled spread is delayed with respect to the free evolution; this is a positive consequence, since it allows a simpler managing of the sanitary emergency. Moreover, it can be evaluated the total number of dead subjects in the population, both with and without the application of the proposed surveillance control strategy; the total number of deaths is equal to 8.85×10^4 without the determined control, whereas is 1.94×10^4 with the determined action that actually produces a decrease of more than 78%. These results show the strong sanitary impact of a suitably planned test campaign. Finally, it is interesting to study the influence of the total number of asymptomatic subjects on the infected isolated and hospitalized patients. It can be noted from the state trajectory of Fig. 8 that, in the absence of an optimal swab test campaign, the number of infected patients (isolated and hospitalized) keeps

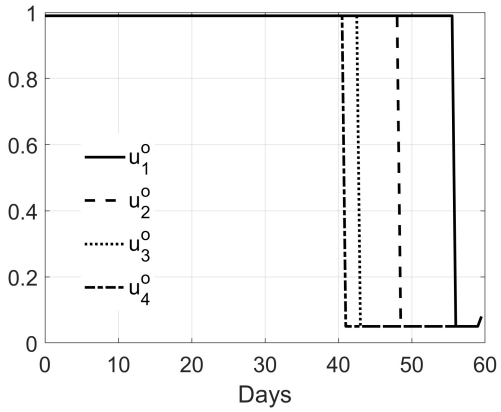

Figure 3: Optimal control strategy.

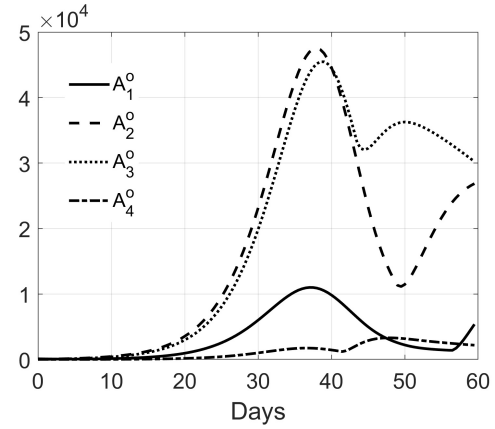

Figure 4: Trend of the asymptomatic subjects in the 4 groups.

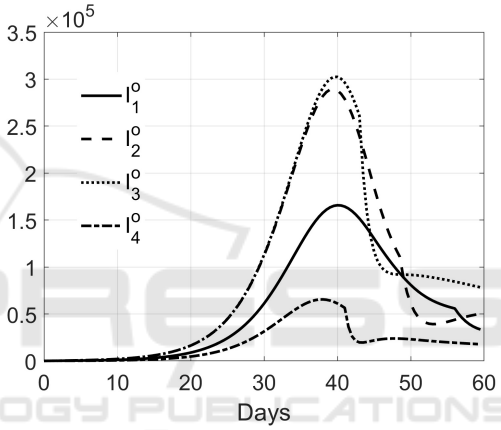

Figure 5: Trend of the infected subjects in the 4 groups.

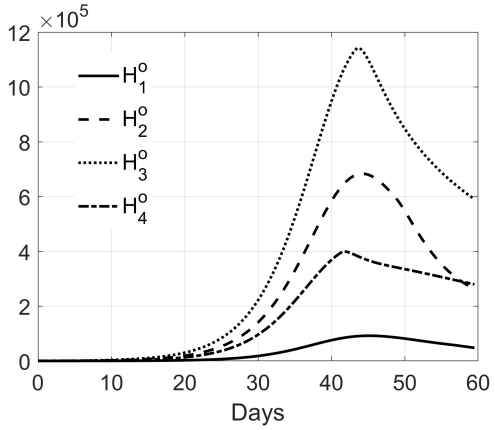

Figure 6: Trend of the hospitalized subjects in the 4 groups.

on increasing even when the number of asymptomatic individuals has started decreasing.

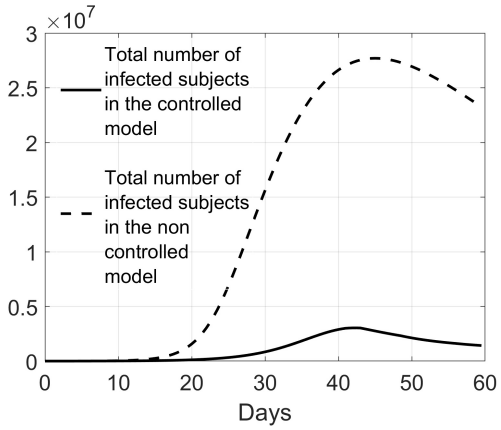

Figure 7: Comparison between the trend of total number of infected patients in the controlled and non controlled conditions.

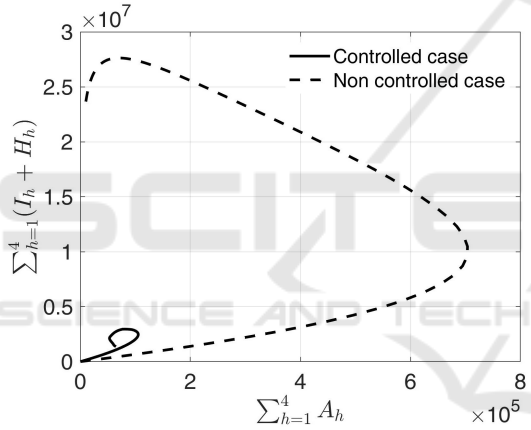

Figure 8: Asymptomatic subjects in the population (that is $\sum_{h=1}^{4}A_h$) versus the sum of infected and hospitalized patients (that is $\sum_{h=1}^{4}(I_h+H_h)$); in continuous line the controlled case, in dashed line the non controlled one.

To stress the potentialities of the approach, it is proposed a second case in which the subjects in G_1 are both more infectious and more susceptible to the infection than the other groups,preserving their general good health, as well as the weak probability of having severe complications. The matrix β representing the new assumption on G_1 is given by

$$\beta = 10^{-7}\begin{pmatrix} 9.5 & 9 & 9 & 9 \\ 9.4 & 8 & 7 & 4 \\ 9.4 & 5 & 8 & 7 \\ 9.8 & 5 & 7 & 8 \end{pmatrix}. \qquad (23)$$

In Fig. 9 it is shown the optimal control strategy for the swab test campaign; all the actions start at their maximal rate but only few days after the beginning of the control period, that is after about 5 days, and they maintain the maximum value for different periods: u_1^o up to day 55, u_2^o up to day 48, u_3^o up to day 40, and u_4^o up to day 37. Using this control strategy that optimizes the swab test campaign, the total number of dead people is reduced more than 79% w.r.t. the uncontrolled case, i.e. from $1.2 \cdot 10^5$, in the absence of any control, to $2.4 \cdot 10^4$, with the application of the optimal strategy.

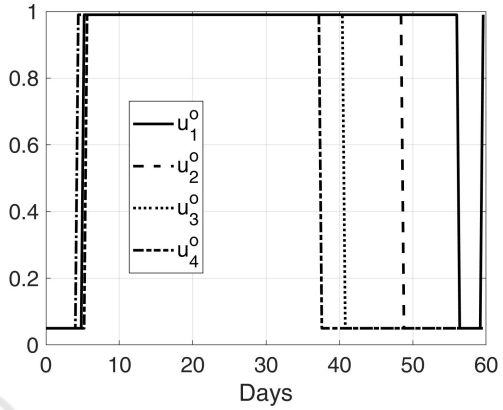

Figure 9: Optimal control strategy for the scenario described by the contact rate matrix (23).

In Fig. 10 it is shown a comparison of the number of infected in the four groups, with and without the application of the swab test campaign; it is evident the strong reduction of the infected patients, especially for the subjects in groups G_2, G_3 and G_4. Similar trends can be observed in Fig. 11 that shows

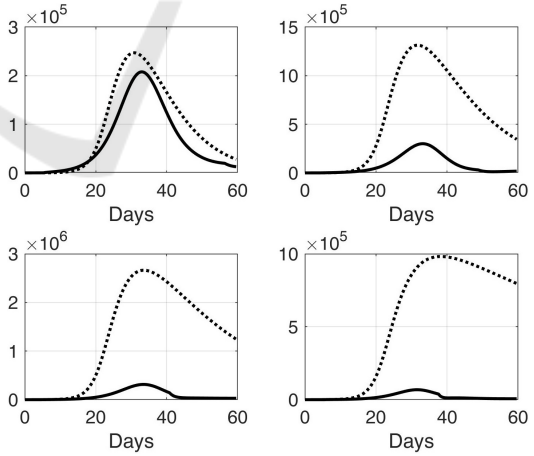

Figure 10: Comparison between I_i^o, $i = 1,...,4$ (Continuous line) and I_i (dotted line) with the contact rate matrix (23); first row, from left to right: infected patients in G_1, G_2; second row, from left to right: infected patients in G_3, G_4.

the comparison between the hospitalized patients with and without the control. The improvements are due to the resource allocation obtained by the optimal swab test campaign that strongly reduces the number

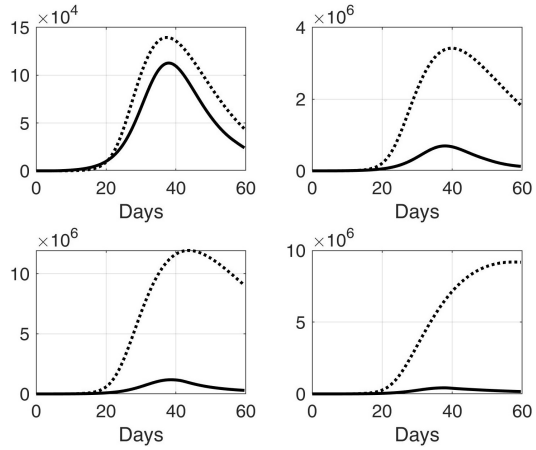

Figure 11: Comparison between H_i^o, $i = 1,...,4$ (Continuous line) and H_i (dotted line) with the contact rate matrix (23); first row, from left to right: hospitalized patients in G_1, G_2; second row, from left to right: hospitalized patients in G_3, G_4.

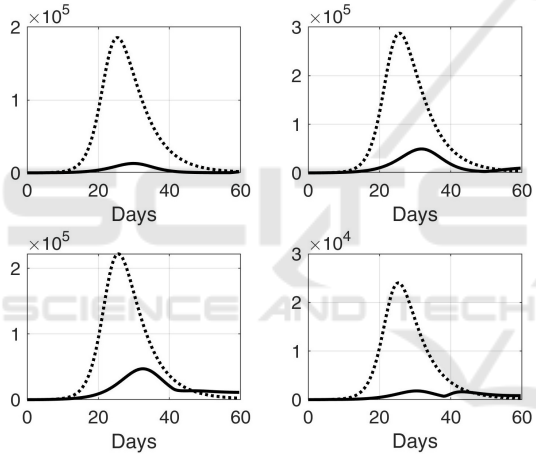

Figure 12: Comparison between A_i^o, $i = 1,...,4$ (Continuous line) and A_i (dotted line) with the contact rate matrix (23); first row, from left to right: asymptomatic subjects in G_1, G_2; second row, from left to right: asymptomatic subjects in G_3, G_4.

of asymptomatic subjects, see Fig.12. The results of Figs. 10, 11, 12 can be summarized in Fig. 13 where it is shown the trend of the infected and infectious individuals both in the controlled and non controlled case; note that there is one order of magnitude of difference in the peaks of the two curves ($3.1 \cdot 10^6$ versus $2.7 \cdot 10^7$ patients). The effect of an effective swab test campaign on the number of asymptomatic individuals, and therefore on the infected isolated patients and on the hospitalized ones, is also highlighted by the state trajectory reported in Fig. 14; note that in the controlled case (continuous line), both asymptomatic subjects and infected patients initially increase but, after a while, they both decrease. Conversely, without any action (dashed line), the number of infected isolated and hospitalized patients remains high even when the number of asymptomatic subjects is actually decreasing.

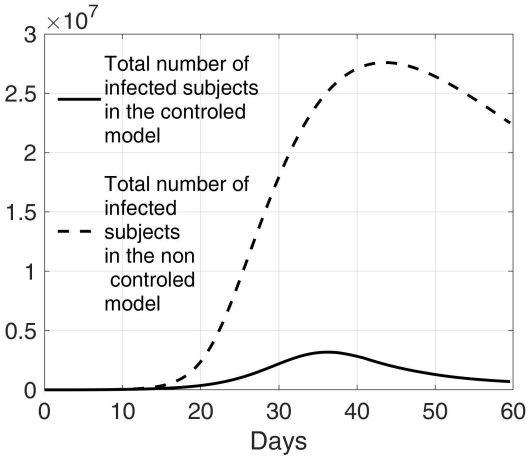

Figure 13: Comparison between the trend of total number of infected patients in the controlled and non controlled conditions in the second case-study.

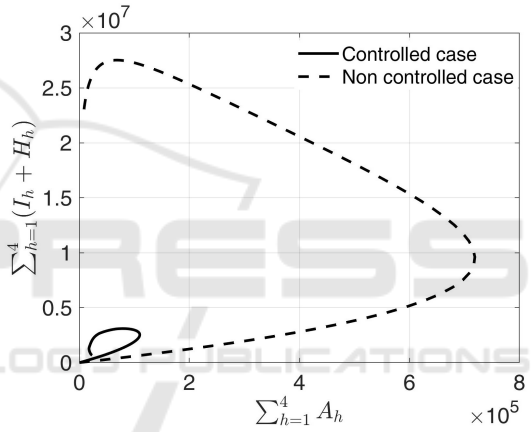

Figure 14: Asymptomatic subjects in the population (that is $\sum_{h=1}^{4} A_h$) versus the sum of the infected and hospitalized patients (that is $\sum_{h=1}^{4}(I_h + H_h)$) in the second case-study; in continuous line the controlled case, in dashed line the non controlled one.

4 CONCLUSIONS

The management of a pandemic, such as that due to Sars-COV 2, must consider various aspects, as the allocation of limited resources from different points of view. The endemic phase also requires attention and active surveillance. In this work, referring to COVID-19, we propose a methodology for the definition of a protocol for the management of swab tests in a population in which different groups can be identified

based on some characteristics (age, work, social condition, etc.). These groups are connected by a network of contacts; their different susceptibility to the virus, infectious capacity and speed of healing suggest an optimal strategy for a swab test campaign. The analysis, supported by the numerical results, suggests a control strategy that particularly focuses on the most infectious individuals, allowing less surveillance on the most fragile subjects. In future work different network population characteristics could be included.

REFERENCES

Assefa, Y., Gilks, C. F., Reid, S., van de Pas, R., Gete, D. G., and Van Damme, W. (2022). Analysis of the COVID-19 pandemic: lessons towards a more efective response to public health emergencies. *Globalization and Health*, 18.

Borri, A., Palumbo, P., Papa, F., and Possieri, C. (2021). Optimal design of lock-down and reopening policies for early-stage epidemics through SIR-D models. *Annual Reviews in control*, 51:511–524.

Casares, M. and Khan, H. (2020). The timing and intensity of social distancing to flatten the COVID-19 curve: The case of Spain. *Int J of Env Res and Pub He*, 1(7283):1–14.

Contreras, S., Villavicencio, H. A., Medina-Ortiz, D., Biron-Lattes, J. P., and Olivera-Nappa, A. (2020). A multi-group SEIRA model for the spread of COVID-19 among heterogeneous populations. *Chaos Solitons Fractals*, 136:109925.

Di Giamberardino, P., Iacoviello, D., Papa, F., and Sinisgalli, C. (2021). A data-driven model of the covid-19 spread among interconnected populations: epidemiological and mobility aspects following the lockdown in italy. *Nonlinear dynamics*, 106(2):1239–1266.

Di Giamberardino, P., Caldarella, R., and Iacoviello, D. (2021a). A control based mathematical model for the evaluation of intervention lines in COVID-19 epidemic spread: The italian case study. *Symmetry*, 13(5):1–21.

Di Giamberardino, P. and Iacoviello, D. (2021). Evaluation of the effect of different policies in the containment of epidemic spreads for the COVID-19 case. *Biomed Signal Process Control*, 65(102325):1–15.

Di Giamberardino, P., Iacoviello, D., Papa, F., and Sinisgalli, C. (2021b). Dynamical evolution of COVID-19 in Italy with an evaluation of the size of the asymptomatic infective population. *IEEE Journal of Biomedical and Health Informatics*, 25(4):1326–1332.

Espinoza, B., Castillo-Chavez, C., and Perrings, C. (2020). Mobility restrictions for the control of epidemics: When do they work? *PLoS One*, 15(7):e0235731.

Gatto, M., Bertuzzo, E., Mari, L., Miccoli, S., Carraro, L., Casagrandi, R., and Rinaldo, A. (2020). Spread and dynamics of the COVID-19 epidemic in Italy: Effects of emergency containment measures. *PNAS*, 117:10484–91.

Ivorra, B., Ferrandez, M. R., Vela-Perez, M., and Ramos, A. M. (2020). Mathematical modeling of the spread of the coronavirus diseas 2019 (COVID-19) taking into account the undetected infections. The case of China. *Communcations in Nonlinear Science and Numerical Simulations*, 88.

Liu, M., Thomadsen, R., and Yao, S. (2020). Forecasting the spread of COVID-19 under different reopening strategies. *Sci Rep.*, 10(1):20367.

Marziano, V., Guzzetta, G., Rondinone, B., Boccuni, F., Riccardo, F., Bella, A., Poletti, P., Trentini, F., Pezzotti, P., Brusaferro, S., Rezza, G., Iavicoli, S., Ajelli, M., and Merler, S. (2021). Retrospective analysis of the italian exit strategy from COVID-19 lockdown. *PNAS*, 118:e2019617118.

Ndairou, F., Area, I., Nieto, J., and Torres, D. (2020). Mathematical modeling of covid-19 transmission dynamics with a case study of wuhan. 135:1–6.

Pung, R., Cook, A., Chiew, C., Clapham, H. E., Sun, Y., Li, Z., Dickens, B., Ma, S., Mak, K., Tan, C., Heng, D., Chen, M., and Lee, V. (2021). Effectiveness of Containment Measures Against COVID-19 in Singapore: Implications for Other National Containment Efforts. *Epidemiology*, 32(1):79–86.

Silva, C. J., Cruz, C., Torres, D. F. M., Munuzuri, A. P., Carballosa, A., Area, I., Nieto, J. J., Pinto, R. F., Passadouro, R., dos Santos, E., Abreu, W., and Mira, J. (2021). Optimal control of the covid-19 pandemic: controlled sanitary deconfinement in portugal. *Scientific Reports*, 11(3451):1–15.

Tang, B., Wang, X., Li, Q., Bragazzi, N. L., Tang, S., Xiao, Y., and Wu, J. (2020). Estimation of the transmission risk of the 2019-nCoV and its implication for public health interventions. *J Clin Med*, 9:462.

Van Den Driessche, P. and Watmough, J. (2002). Reproduction numbers and sub–threshold endemic equilibria for compartmental models of disease transmission. *Mathematical Biosciences*, 180:29–48.

Wang, B., Xu, S., and Mansouri, M. (2020). Modeling the emergence of COVID-19: a system approach. In *IEEE 15th International Conference of System of Systems Engineering*.

Wu, J. T., Leung, K., and Leung, G. M. (2020). Nowcasting and forecasting the potential domestic and international spread of the 2019-nCoV outbreak originating in Wuhan, China: a modelling study. *Lancet*, 395:689–697.